Journal of Alloys and Compounds 509 (2011) 4553–4556

Contents lists available at ScienceDirect

Journal of Alloys and Compounds

journal homepage: www.elsevier.com/locate/jallcom

Effect of small oxygen deficiency on the para-coherent transition and 2D–3D crossover in untwinned $YBa_2Cu_3O_{7-\delta}$ single crystals

R.V. Vovk[a], Z.F. Nazyrov[a], M.A. Obolenskii[a], I.L. Goulatis[a], A. Chroneos[b,*], V.M. Pinto Simoes[c]

[a] Kharkov National University, 4 Svoboda Sq., 61077 Kharkov, Ukraine
[b] Department of Materials, Imperial College, London SW7 2AZ, United Kingdom
[c] IPA Instituto Superior Autónomo de Estudos Politécnicos, Rua de Xabregas, 20, 1° 1900-440 Lisboa, Portugal

ARTICLE INFO

Article history:
Received 1 October 2010
Received in revised form 10 January 2011
Accepted 15 January 2011
Available online 22 January 2011

Keywords:
Excess conductivity
$YBa_2Cu_3O_{7-\delta}$ single crystals
Oxygen deficit
Pinning
2D–3D crossover
Coherent length

ABSTRACT

We investigate the influence of the disorientation angle between the direction of a constant magnetic field (up to 15 kOe) and the ab-plane $\alpha \equiv \angle(\mathbf{H},ab)$ to the temperature dependence of the excess conductivity in the temperature interval of the transition to the superconducting state in untwinned $YBa_2Cu_3O_{7-\delta}$ single crystals. We discuss the appearance of low temperature "tails" (para-coherent transitions) on the resistive transitions, corresponding to different phase regimes of the vortex-matter state. At temperatures above the critical temperature, the temperature dependence of the excess para-conductivity is interpreted within the Hikami–Larkin theoretical model of the fluctuation conductivity for layered superconductors.

1. Introduction

The study of functional materials with high current-carrying capacity is an important field of the physics of high-temperature superconductivity (HTSC). The model high temperature HTSC remains the $ReBa_2Cu_3O_{7-\delta}$ (Re = Y or rare earth ion) system. Defects, the composition or external means such as pressure can be significant for tuning the properties of $ReBa_2Cu_3O_{7-\delta}$ [1–14]. For example, $HoBa_2Cu_3O_{7-\delta}$ is paramagnetic in the normal state, whereas $YBa_2Cu_3O_{7-\delta}$ is not (refer to [8] and references therein). An example of external means to optimize the properties of these materials include recent studies that attempted to elucidate the effect of high pressure on properties such as the fluctuation conductivity, the pseudo-gap and the charge transfer [6,13]. In HTSC a small coherence length ξ and a large penetration depth λ can result in the effective pinning of point defects such as oxygen vacancies and dopant atoms [2–4]. The impact of such defects on the phase state of the vortex matter is often difficult to explain due to the presence of intergranural boundaries, twin boundaries (TB), defect clusters and other powerful pinning centers. Intrinsic pinning due to the layered structure of HTSC compounds can also impact the results [3].

In the present study we investigate the magnetic conductivity in untwined $YBa_2Cu_3O_{7-\delta}$ single crystals under a fixed magnetic field and different values of the angle (α) between the magnetic field H and the ab-plane (**H**,*ab*). We use untwined single crystals to eliminate the influence of intergranural boundaries and TB. This allows the selected experimental geometry to determine the contribution of intrinsic pinning.

In $YBa_2Cu_3O_{7-\delta}$ compounds the oxygen stoichiometry influences the concentration of point defects [15]. The measurement of the resistivity transitions (they are sensitive to concentration changes) to the superconducting state allows the investigation of the impact of the point defects to the phase state and to the dynamics of vortex matter. This can be achieved by the analysis of the influence of fluctuations on the conductivity observed in HTSC compounds at temperatures near to the critical temperature ($T \approx T_c$) [16].

2. Experimental techniques

The $YBa_2Cu_3O_{7-\delta}$ single crystals were grown in a gold crucible with the solution-melting method [15]. The $YBa_2Cu_3O_{7-\delta}$ oxygen saturating regime leads to the tetra–ortho structural transition, which results to the crystal twinning in order to minimize its elastic energy. To obtain untwined samples, we used a special cell at a temperature of 420 °C and pressure 30–40 GPa. This is in similar to the procedure of Giapintzakis et al. [17]. To obtain oxygen stoichiometric samples, the crystal was annealed again in an oxygen flow at a temperature of 420 °C for a period of seven days.

To form electric contacts the standard four-contact scheme was used. Silver paste was applied on the surface of the crystal and the connection of silver conduc-

* Corresponding author. Tel.: +30 6978775320.
E-mail addresses: Ruslan.V.Vovk@univer.kharkov.ua (R.V. Vovk), alexander.chroneos@imperial.ac.uk (A. Chroneos).

0925-8388/$ – see front matter © 2011 Elsevier B.V. All rights reserved.
doi:10.1016/j.jallcom.2011.01.102

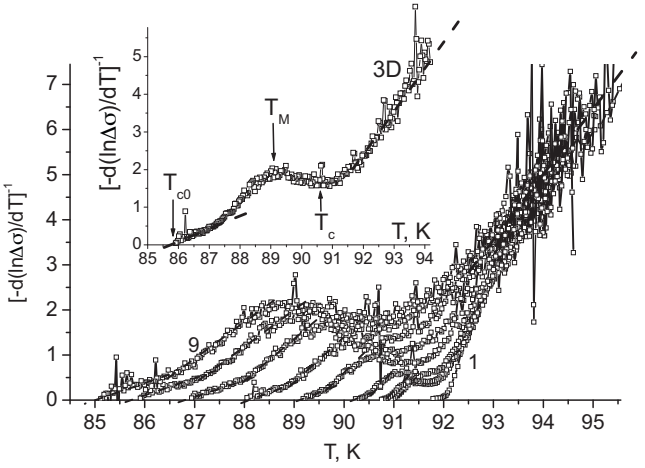

Fig. 1. Resistivity transitions to the SC state for the $YBa_2Cu_3O_{7-\delta}$ single crystal, measured under magnetic field **H** = 0 (curve 1) and for **H** = 15 KOe for different angles $\alpha \equiv \angle(\mathbf{H},ab)$: 0; 5; 10; 20; 30; 45; 60 and 90° (curves 2–9 respectively) in $[-d(\ln\Delta\sigma)/dT]^{-1} - T$ coordinates. In the inset of Fig. 1, the curve obtained for $\alpha = 60°$. The dash lines correspond to the extrapolation of the areas corresponding to various FC regimes. Arrows indicate the characteristic temperatures T_{c0}, T_M and T_c, corresponding to the end of the resistive transition in SC state, the melting point of the vortex lattice and the critical temperature in the mean-field approximation respectively.

tors (with diameter 0.05 mm). Subsequently we annealed for 3 h at a temperature of 200 °C in an oxygen atmosphere. This resulted in contacts with resistance less than 1 Ω and allowed measurements with a current of 10 mA in the *ab*-plane. All the measurements were performed in the temperature drift mode using the method for two opposite directions of the transport current. This practically eliminated the impact of the parasitic signal. A platinum thermo-resistor was used to monitor the temperature, whereas the voltage was measured across the sample and the reference resistor with V2-38 nano-voltmeters. The critical temperature (T_c) was defined as the temperature corresponding to the main maximum in the $d\rho_{ab}(T)/dT$ dependence in the superconductive transition [18]. To produce oxygen hypostoichiometric samples, the crystal was annealed in an oxygen flow, at a temperature of 650 °C for 48 h. The measurements were performed 7 days after the annealing in order to avoid the influence of the relaxation effects. A magnetic field of 15 kOe was created by an electromagnet, which could vary the orientation of the field relative to the crystal. The accuracy of the field orientation relative to the sample was better than 0.2°. A bridge was mounted in the measuring cell so that the vector field **H** was always perpendicular to the vector of the transport current *j*.

3. Results and discussion

For investigations of the resistive transitions in superconducting (SC) state we used the Kouvel–Fischer method [19]. This is based on the analysis of the quantity $\chi = (-d(\ln\Delta\sigma))/dT$, where $\Delta\sigma = \sigma - \sigma_0$ is the excess conductivity. The excess conductivity arises in the conducting subsystem due to the fluctuation pairing of carriers at $T > T_c$ [20] and can be determined by the phase state of vortex matter at $T < T_c$ [16]. Here $\sigma = \rho^{-1}$ is the experimentally measured value of conductivity, and $\sigma_0 = \rho_0{}^{-1} = (A + BT)^{-1}$ is a term, determined by extrapolating the high-temperature linear segment up to the area of the SC transition. Assuming that $\Delta\sigma$ diverges as $\Delta\sigma \sim (T - T_c)^{-\beta}$ at $T \approx T_c$, from the derivative $\chi = (-d(\ln\Delta\sigma))/dT$ it follows that $\chi^{-1} = \beta^{-1}(T - T_c)$, where β depends on the dimension and the phase state of the fluctuation and vortex subsystems [16,20]. The identification of linear temperature dependence of $\chi^{-1}(T)$ allows the determination of important dimensional parameters and characteristic temperatures of dynamic phase transitions in the SC carriers subsystem.

Fig. 1 represents the resistivity transitions to the SC state, measured under **H** = 0 (curve 1) and for a fixed magnetic field of **H** = 15 KOe for different angles $\alpha \equiv \angle(\mathbf{H},ab)$ (curves 2–9). The inset of Fig. 1 represents the curve obtained for $\alpha = 60°$. This indicates the characteristic temperatures T_{c0}, T_M and T_c, corresponding to the end of the resistive transition in SC state, the melting point of the vortex lattice and the critical temperature in the mean-field approximation respectively [3,16,18]. In all curves in the high-temperature area of the SC transition we observe a linear region with slope $\beta \approx 0.5$. This according to Aslamazov–Larkin [20] indicates the realization of a three-dimensional (3D) regime of the fluctuation carriers existence in the system. In this, the section corresponding to 3D regime is essentially unstable in the magnetic field. This is consistent with the results obtained by Costa et al. [16]. When increasing the temperature from T_c upwards, an increase of the absolute value of β occurs suggesting the realization of a 3D–2D crossover in the system (see below for details). The application of magnetic field and the increase of the angle α, leads to a significant expansion of the SC transition in comparison with the sharp ($\Delta T_c \approx 0.3$ K) transition observed at **H** = 0.

A significant transformation of the form of the SC-transition occurs, which is expressed in the appearance of an additional low-temperature peak. This peak rapidly shifts downwards to lower temperatures as the angle α increases with a simultaneous increase of the width and the amplitude of the peak. Notably, this expansion of the SC transition is three times more substantial than the expansion observed in stoichiometric untwinned $YBa_2Cu_3O_{7-\delta}$ single crystals [3] measured at the same value of magnetic field and with a similar experimental geometry.

Kwok et al. [3] observed a sharp "kink", which they explained by the appearance of first-order phase transition, corresponding to the melting of the vortex lattice. It is established [2,3], that the presence of strong pinning centers in the system, leads to a spreading of the kink and the transition from an ordered vortex-lattice phase to a phase, so-called "vortex" or "Bragg" glass in which the vortex system is accommodated in the chaotic pinning potential. This chaotic pinning potential violates the long-range order of vortex lattice, thereby suppressing the first-order phase transition and results to the formation of the glassy state of vortices. In the resistive transitions there appear "tails", whose amplitude is less than the resistance of viscous flow (ρ_{ff}). These are probably due to a partial pinning of the vortex liquid.

Clusters of oxygen vacancies could also have a significant role. Previously we investigated the influence of annealing at room temperature on the excess conductivity for the same samples [21]. Immediately after annealing in oxygen atmosphere at temperature of 500 °C the crystal had a critical temperature $T_c \cong 91.75$ K with a transition width $\Delta T_c \cong 0.3$ K. Thereafter, the crystal was retained at room temperature for a week. As it was demonstrated previously, this led to a decrease in electrical resistance in the normal state $\rho(300\,K)$ of ≈3% and an increase in $T_c \approx 0.25$ K. These changes are consistent with the concept of formation of clusters of oxygen vacancies in the process of ordering the vacancy subsystem [21]. This will effectively lead to an increase in the oxygen concentration in the crystal and a decrease in the oxygen content in the region of the clusters. In turn, there is a decrease in the concentration of carriers scattering centers in the volume of the crystal and a reduction of the resistance $\rho(300\,K)$.

Taking into consideration the dome-shaped dependence T_c from carrier concentration, with a maximum value of $T_c \cong 93$ K at $\delta \cong 0.93$ [22], we can assume that the redistribution of the labile oxygen leads to phase separation in the crystal and the formation of phase clusters with different values of T_c. Considering the presence of percolation paths of current flow on the main volume of the crystal, this process, should lead to an increase in the measured value of T_c. In the single crystal there coexists a point pinning potential created by the isolated oxygen vacancies and a volume pinning potential with a suppressed superconducting order parameter, formed by the clusters of oxygen vacancies. Costa et al. [16] determined that in the case of "Bragg glass" state the dependence $\chi(T)$ can be scaled in $\chi(T_c - T_{c0}) - (T - T_{c0})/(T_c - T_{c0})$ coordinates. In this, T_{c0} is

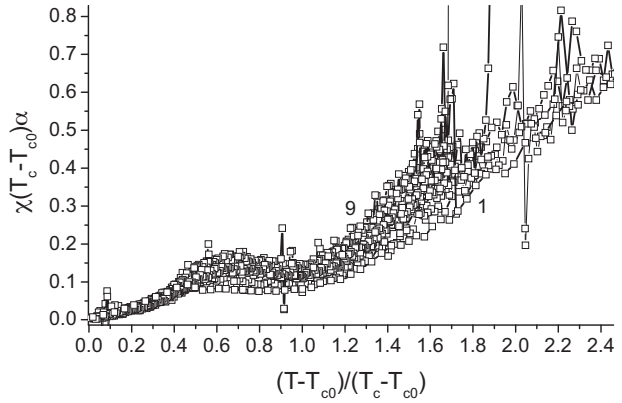

Fig. 2. Resistivity transition to the SC state for the $YBa_2Cu_3O_{7-\delta}$ crystal in (reducing) $\chi(T_c - T_{c0})/\alpha$ versus $(T - T_{c0})/(T_c - T_{c0})$ coordinates. The numbering of the curves is consistent to Fig. 1.

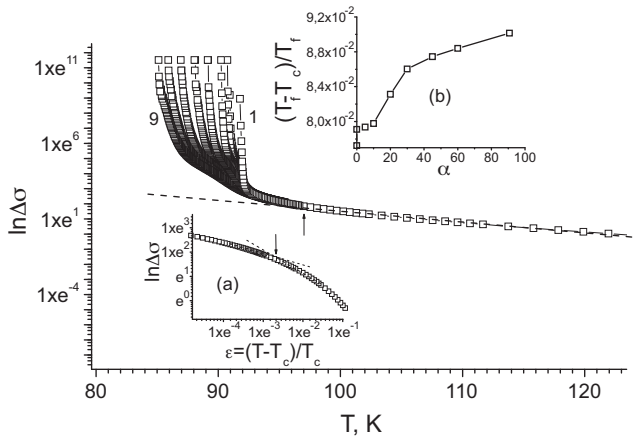

Fig. 3. Plot of the temperature dependence of the excess conductivity for the $YBa_2Cu_3O_{7-\delta}$ single crystal in ab-plane in ln $\Delta\sigma - T$ coordinates. The numbering of the curves is consistent to Fig. 1. The dash line corresponds to the approximation of the areas to the PG regime and the arrows shows the transition point to the FC regime. In the inset (a): the temperature dependence of the excess conductivity in $\ln\Delta\sigma - \ln\varepsilon$ coordinates, under magnetic field $\mathbf{H} = 0$. The dash lines correspond to the approximation of the experimental curves with slope $tg\beta 1 \approx -0.5$ (3D regime) and $tg\beta 2 \approx -1.0$ (2D regime). The arrow indicates the 2D–3D crossover point. In the inset (b): the relative spread of FC regime's: $t_f = (T_f - T_c)/T_c$.

the critical temperature of the transition in the para-coherent area, determined at the point of intersection with the linear interval, approximating the so called para-coherent area with the temperature axis. T_c is the temperature corresponding to the mean-field critical temperature, determined as the maximum in the curves $d\rho_{ab}(T)/dT$ [18].

We account for the change of the self-pinning contribution with the increase of the disorientation angle $\alpha \equiv \angle(\mathbf{H},ab)$, by introducing the reduced value $\chi(T_c - T_{c0})/\alpha$. In Fig. 2, the best scaling in the experimental curves is observed in the para-coherent area at $T < T_M$. At higher temperatures, the spread in the curves becomes significant, and this can be due to the influence of the pinning of superconducting fluctuations on the cluster inclusions.

Above T_c there are peculiarities related to crossover between various fluctuation conductivity (FC) regimes. According to Hikami and Larkin [23], the general expression for the fluctuation paraconductivity $\Delta\sigma(T,H)$ of layered superconductors in magnetic field can be described by the following expression:

$$\Delta\sigma(T,H) = \Delta\sigma_{AL}(T,H) + \Delta\sigma_{MT}(T,H) \quad (1)$$

where

$$\Delta\sigma_{AL}(T,H) = \frac{e^2}{16\hbar d\varepsilon}\left\{\frac{1}{(1+2\alpha)^{1/2}} - \frac{(2+4\alpha+3\alpha^2)}{4(1+2\alpha)^{5/2}}\frac{b^2}{\varepsilon^2} + \cdots\right\} \quad (2)$$

is the fluctuation conductivity Aslamazov–Larkin [20] and

$$\Delta\sigma_{MT}(T,H) = \frac{e^2}{8\hbar d(1-\alpha/\delta)\varepsilon}\left\{\ln\left(\frac{\delta}{\alpha}\frac{1+\alpha+\sqrt{1+2\alpha}}{1+\delta+\sqrt{1+2\delta}}\right) - \left[\frac{\delta^2}{\alpha^2}\frac{1+\delta}{(1+2\delta)^{3/2}} - \frac{1+\alpha}{(1+2\alpha)^{3/2}}\right]\frac{b^2}{6\varepsilon} + \ldots\right\} \quad (3)$$

is the fluctuation conductivity Maki–Thompson [24], due to the interaction of unpaired carriers with the fluctuation Cooper pairs; d is the thickness of the two-dimensional layer, $\varepsilon = (T - T_c)/T_c$ is the reduced temperature; $\alpha = 2\xi_c^2(0)/d^2\varepsilon$; $b = (2e\xi_{ab}^2(0)/\hbar H$; $\delta = (16/\pi)(\xi_c^2(0)/d^2)(kT\tau_\varphi/\hbar)$; $\xi_{ab}(0)$ is the coherence length in the basic plane, and τ_φ is the typical failure term of the order parameter.

For $\xi_c(0) \approx 2$ Å, $d \approx 11.7$ Å [25], $\tau_\varphi \approx \hbar/2k_BT_c$, we can estimate the evolution of the relative contribution of each part of Eq. (1) $\Delta\sigma_{AL}/\Delta\sigma_{MT}$ as we increase the temperature from the transition to the SC state point in zero magnetic field [26]. The analysis of Eq. (2) and Eq. (3) demonstrates that although within the temperature range $T_c < T < 1.1T_c$ the component $\Delta\sigma_{MT}(T, H = 0)$ when compared with $\Delta\sigma_{AL}(T, H = 0)$ is depending significantly less from the temperature. Notably, the $\Delta\sigma_{AL}/\Delta\sigma_{MT}$ ratio decreases by more than twice when the temperature increases from $1.005T$ to $1.1T$. This indicates a significant increase in the scattering intensity of Cooper pairs by the normal carriers.

Notably, all the $\Delta\sigma(T,H)$ dependencies in the temperature interval 1.08–1.2 T_c (inset (a) to Fig. 3) can be approximated by the dependence:

$$\Delta\sigma_D = A_D\varepsilon^{-\beta}, \quad (4)$$

for the two-dimensional case ($A_{2D} = (e^2)/(16\hbar d)$ and $\beta \approx -1$ [20]). When $T < 1.08T_c$ the behavior of $\Delta\sigma(T,H)$ is in agreement with Eq. (4) regarding the 3-dimensional case $A_{3D} = (e^2)/(32\hbar\xi_c(0))$ and $\beta \approx -1.2$ [20]). From Eq. (4), in the 2D–3D crossover:

$$\xi_c(0)\varepsilon_0^{-1/2} = \frac{d}{2} \quad (5)$$

The value of $\xi_c(0)$ can be calculated by determining the value ε_0 at the intersection of two the lines corresponding to the exponent of −0.5 and −1 in the $\ln\Delta\sigma - \ln\varepsilon$ curves respectively and using the literature data regarding the interplanar distance dependence from δ [25] ($d \approx 11.7$ Å). Fig. 3(a) shows the temperature dependence $\Delta\sigma(T)$ in $\ln\Delta\sigma - \ln\varepsilon$ coordinates. Near T_c these dependences are well approximated by lines with slope $tg\beta 1 \approx -0.5$, which corresponds to the exponent index – ½ in Eq. (4). This reveals a 3D nature of the fluctuation superconductivity in this temperature interval. As the temperature increases, the slope of $\Delta\sigma$ significantly increases ($tg\beta 2 \approx -1$). This can be considered as a change in the dimension of the fluctuation conductivity. The calculations indicate that in the process of changing, the disorientation angle $\alpha \equiv \angle(\mathbf{H},ab)$ there is no significant change in the value of the coherence length (which, in our case is $\xi_c(0) \approx 1.68 \pm 0.03$ Å).

The Density of States (DOS) fluctuations can provide information on the emergence and evolution of the excess conductivity $\Delta\sigma$ in layered HTSC structures. Nevertheless, the impact of such fluctuations is strongly manifested at temperatures considerably above the critical temperature, $T \gg T_c$ [26–28]. Previous studies [27–29] determined that in this temperature interval, the appearance of $\Delta\sigma$ is mainly due to the realization of the pseudo-gap (PG) anomalies. The present experimental data indicates that a constant magnetic field has no significant effect on the temperature dependence $d\rho_{ab}(T)$ and $\Delta\sigma(T)$ at $T > 1.2T_c$. This is consistent with previous experiments in related compounds [26]. The application of a constant magnetic field does not shift the temperature

T^*, which is the point where the deviation from linearity in the $\rho_{ab}(T)$ dependence is observed. The temperature T^* corresponds to the temperature that the PG commences [27,28]. In the present study we have not considered the DOS fluctuations. If we define the temperature of transition to the FC regime T_f on the point of deviation of the values $\ln\Delta\sigma$ upwards the linear dependence $\ln\Delta\sigma(T)$ [27] (see inset (b) to Fig. 3), we can estimate the relative spread of FC regime's existence as: $t_f = (T_f - T_c)/T_c$. The calculations show that increasing the disorientation angle $\alpha \equiv \angle(\mathbf{H},ab)$ a total relative expansion of the temperature interval in which the fluctuation para-conductivity regime is realized from $t_f \approx 0.8589$ at $\alpha = 0$ to $t_f \approx 0.9991$ at $\alpha = 90^\circ$. This is probably due to the suppression from α of the so-called "beyond 3D" regime and the increase of the long-wavelength fluctuations. These have a very significant contribution to the para-conductivity near T_c. In previous work [27], it was determined that the underestimation of the contribution of the short-wave order parameter fluctuations leads to a faster (in comparison to the theoretical predictions) decrease in the $\Delta\sigma$, with a sufficiently large displacement from the T_c upwards the higher temperatures. The microscopic computation of the fluctuation amendment to the conductivity taking into account all the components of the order parameter was carried out in the work of Reggani et al. [28]. Comparing our data with the theoretical work [28] demonstrates that, as in the case of undoped $YBa_2Cu_3O_{7-\delta}$ films [27], the $\Delta\sigma$ can be described within the improved theory of FC at temperatures, close to 1.25 T_c. In this temperature interval the transition to the pseudo-gap regime commences consistently to recent analysis [29].

4. Conclusions

The application of a constant magnetic field to $YBa_2Cu_3O_{7-\delta}$ single crystals with a small oxygen hypostoichiometry (in distinction to similar stoichiometric samples) leads to an additional para-coherent transition in the excess conductivity temperature dependences in the basic *ab*-plane in the area of the resistive transition to the SC state. Increasing the angle $\alpha \equiv \angle(\mathbf{H},ab)$ leads to an increase of the amplitude and the width of the peak, corresponding to this transition, and its shift to the area of lower temperatures. This can be due to a decrease of the self intrinsic pinning of the vortex subsystem contribution with the increase of α and the strengthening the role of volume pinning due to the presence of clusters of oxygen vacancies in the experimental sample. Consequently, at temperatures below the critical ($T < T_c$) there is a suppression of the dynamic phase transition type liquid vortex–vortex lattice and the formation of transition in the system type liquid vortex–vortex "Bragg" glass. The FC near T_c is described by the 3D Aslamazov–Larkin model for layered superconducting systems. The increase in disorientation angle $\alpha \equiv \angle(\mathbf{H},ab)$ results to an increase of the temperature interval that the fluctuation para-conductivity regime is realized. This can be due to the increase of the role of the long-wavelength fluctuations of the order parameter.

References

[1] A. Chroneos, R.V. Vovk, I.L. Goulatis, L.I. Goulatis, J. Alloys Compd. 494 (2010) 190.
[2] A.V. Bondarenko, A.A. Zavgorodniy, D.A. Lotnik, M.A. Obolenskii, R.V. Vovk, E.V. Biletskiy, Low Temp. Phys. 34 (2008) 645.
[3] W.K. Kwok, S. Fleshler, U. Welp, V.M. Vinokur, J. Downey, G.B. Crabtree, M.M. Miller, Phys. Rev. Lett. 69 (1992) 3370.
[4] A.A. Zavgorodniy, R.V. Vovk, M.A. Obolenskii, A.V. Samoilov, Low Temp. Phys. 36 (2010) 143.
[5] U. Topal, M. Akdogan, J. Alloys Compd. 503 (2010) 1.
[6] R.V. Vovk, M.A. Obolenskii, A.A. Zavdorodniy, A.V. Bondarenko, I.L. Goulatis, A.V. Samoilov, A. Chroneos, J. Alloys Compd. 453 (2008) 69.
[7] R.K. Singhal, J. Alloys Compd. 495 (2010) 1.
[8] R.V. Vovk, M.A. Obolenskii, A.A. Zavdorodniy, I.L. Goulatis, A. Chroneos, E.V. Biletskiy, J. Alloys Compd. 485 (2010) L21.
[9] N.H. Ahmad, N.A. Khan, A.K. Yahya, J. Alloys Compd. 492 (2010) 473.
[10] A. Kortyka, R. Puzniak, A. Wisniewski, H.W. Weber, C.Y. Tang, X. Yao, K. Conder, Physica C 470 (2010) S217.
[11] R.V. Vovk, M.A. Obolenskii, A.A. Zavdorodniy, I.L. Goulatis, V.I. Beletskii, A. Chroneos, Physica C 469 (2009) 203.
[12] M.F. Bakar, A.K. Yahya, J. Alloys Compd. 490 (2010) 358.
[13] R.V. Vovk, A.A. Zavdorodniy, M.A. Obolenskii, I.L. Goulatis, A. Chroneos, V.M. Pinto Simoes, J. Mater. Sci.: Mater. Electron. 22 (2011) 20.
[14] A.A. Khurram, N.A. Khan, M. Mumtaz, Physica C 469 (2009) 279.
[15] R.V. Vovk, M.A. Obolenskii, A.V. Bondarenko, I.L. Goulatis, A.V. Samoilov, A. Chroneos, V.M. Pinto Simoes, J. Alloys Compd. 464 (2008) 58.
[16] R.M. Costa, I.C. Riegel, A.R. Jurelo, J.L. Pimentel Jr., J. Magn. Magn. Mater. 320 (2008) 493.
[17] J. Giapintzakis, D.M. Ginzberg, P.D. Han, J. Low Temp. Phys. 77 (1989) 155.
[18] L. Mendonca Ferreira, P. Pureur, H.A. Borges, P. Lejay, Phys. Rev. B 69 (2004) 212505.
[19] J.S. Kouvel, M.E. Fischer, Phys. Rev. 136 (1964) 1616.
[20] L.G. Aslamasov, A.I. Larkin, Fiz. Tverd. Tela (Leningrad) 10 (1968) 1104 [Sov. Phys.Solid State 10 (1968) 875].
[21] R.V. Vovk, M.A. Obolenskii, A.A. Zavgorodniy, A.V. Bondarenko, I.L. Goulatis, N.N. Chebotaev, Low Temp. Phys. 33 (2007) 931.
[22] J.L. Tallon, C. Berbhard, H. Shaked, R.L. Hitterman, J.D. Jorgensen, Phys. Rev. B 51 (1995) 12911.
[23] S. Hikami, A.I. Larkin, Mod. Phys. Lett. B 2 (1988) 693.
[24] J.B. Bieri, K. Maki, R.S. Thompson, Phys. Rev. B 44 (1991) 4709.
[25] G.D. Chryssikos, E.I. Kamitsos, J.A. Kapoutsis, A.P. Patsis, V. Psycharis, A. Kafoudakis, C. Mitros, G. Kallias, E. Gamari-Seale, D. Niarchos, Physica C 254 (1995) 44.
[26] N.E. Alexeevskii, A.V. Mitin, E.P. Khlybov, G.M. Kuzmicheva, V.I. Nizankovskii, Supercond.: Phys. Chem. Eng. 2 (1989) 40.
[27] D.D. Prokofyev, M.P. Volkov, Y.A. Boiko, Fiz. Tverd. Tela 45 (2003) 1168.
[28] L. Reggani, R. Vaglio, A.A. Varlamov, Phys. Rev. B 44 (1991) 9541.
[29] R.V. Vovk, M.A. Obolenskiy, A.A. Zavgorodniy, D.A. Lotnyk, K.A. Kotvitskaya, Physica B 404 (2009) 3516.